CAMCOS
Center for Applied Mathematics, Computation and Statistics
Department of Mathematics
San Jose State University
San Jose, CA
June 2006

Mathematical Modeling, Numerical Simulation and Statistical Optimization of Heat Pipe Design

CAMCOS Team

Sergio de Ornelas
Sandra de Sousa
Cuong Dong
Michelle Fernelius
Marian Hofer
Tracy Holsclaw
Adam Jennison
Diem Mai
Kim Ninh
Misako van der Poel

Faculty Supervisors

Dr. Bem Cayco
Dr. Bee Leng Lee

This version of the report has been edited for the SJSU Foundation.
Some parts of this report are confidential and have been deleted.
The original and complete report has been sent to the industry sponsor.

Acknowledgements

We would like to thank

Dr. David Blockus
Dr. Tim Hsu
Dr. Sridhar V. Machiroutu
Dr. Himanshu Pokharna

and our family and friends
for their support.

Table of Contents

Abstract

Heat pipes are extensively used in modern laptops as part of a cooling system that carries heat away from high power components such as a CPU to heat sinks where thermal energy may be dissipated into the environment. The physical phenomenon in the heat pipe is modeled using a system of nonlinear differential equations. Numerical simulation was used to investigate the relationship between manufacturing design parameters and the thermal resistance. Statistical analysis was used to obtain optimal design parameters that minimized the thermal resistance.

I. What is a heat pipe?

A. Introduction

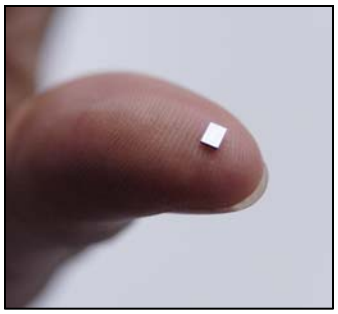

Laptops are truly a modern day marvel. Not only are they getting smaller, thinner, faster, and lighter, but they are also becoming more powerful. The drawback, however, is that these more powerful processors are created by packing more and more tiny transistors onto the same microchip such that, if current trends continue, the circuit elements on a chip should reach the size of a single atom within the next three decades. But hundreds of millions of transistors working in tandem in a small, confined space creates an excessive amount of heat. Without proper cooling, temperatures inside the laptop would rise to a point that would endanger the sensitive electronic components inside.

A heat sink is the conventional way of cooling the CPU. Fins are used to spread the heat across a greater surface area and a fan is used to move the heat out of the computer through forced convection. However such a set up is very space consuming, and would not fit in the modern day laptop, especially with the advances that keep making them thinner. Hence, relocating the heat sink and the fan to a less congested part of the laptop is a reasonable compromise. One must then deal with the problem of transporting the heat from the CPU to the fan set up.

Solid metal rods fall short in this area of heat transportation, simply because they lose so much heat to the environment along the way. This loss of heat energy across the rod as a whole endangers electronic components as much as having no cooling system at all. Having some sort of powered system for moving heat would be counter-productive, as power consumption created the problem in the first place.

So we are looking for a device that can perpetually, without power, transport heat from one location to another, with little to no heat lost to the environment. Fortunately, such a device exists! It is called a heat pipe.

Heat pipes have been around since the 1800's when Jacob Perkins and his company developed the Perkins tube which was used to transfer heat from a furnace to a boiler. In 1944, Gaugler introduced one of the key components of a modern heat pipe, known as the wick structure, allowing the heat pipe to work against gravity. Although the basics of the heat pipe were finalized with this contribution, the scientific community did not realize its full potential until Grover published his research in 1964, showing that this device has a higher thermal conductivity than any known metal. From this research, he coined the term "heat pipe".

In addition to applications in the electronics industry, heat pipes can be found on satellites in space and even along the Alaska pipeline. The vertical heat pipes are used to prevent the permafrost layer along the Alaska pipeline from melting which could cause the support columns to sink, thus damaging the pipeline. In essence, a heat pipe operates as a heat pump, transporting heat from one end to another where the heat can dissipate.

B. The components of a heat pipe: the container, the working fluid and the wicking structure

A heat pipe is a sealed tube which contains a working fluid and a wicking structure. One end is positioned close to a heat source which heats up the working fluid and turns it into vapor. The vapor then travels through the pipe to the other end where a heat sink cools it down and condenses back into its liquid state. The wicking structure enables the cooled liquid to travel back to the heat source through capillary forces. This process is continuously ongoing as long as there is a difference in temperature between these two ends.

The container is usually made of copper or aluminum and can be bent or flattened to conform to an application with a limited amount of space in the laptop. The working fluid is responsible for the transport of heat through the heat pipe. Pure fluids are used as working fluids in heat pipes. Impure fluids can cause deposits in the heat pipe, thereby affecting its overall performance. The type of liquid depends on the temperature range of the application. For example, ammonia, which has a useful range of -60 to 100 °C, is used on the Alaska pipeline heat pipes while water or ethanol is commonly used for laptops.

The wicking structure is the element responsible for the return of liquid from the condenser section to the evaporator section. It is a porous medium which facilitates the movement of fluid through capillary force. Capillary fluid movement is achieved when the intermolecular adhesive forces between a fluid and a solid are greater than the cohesive forces within the fluid itself. This results in an increase in surface tension on the fluid and a force is applied causing the fluid to move.

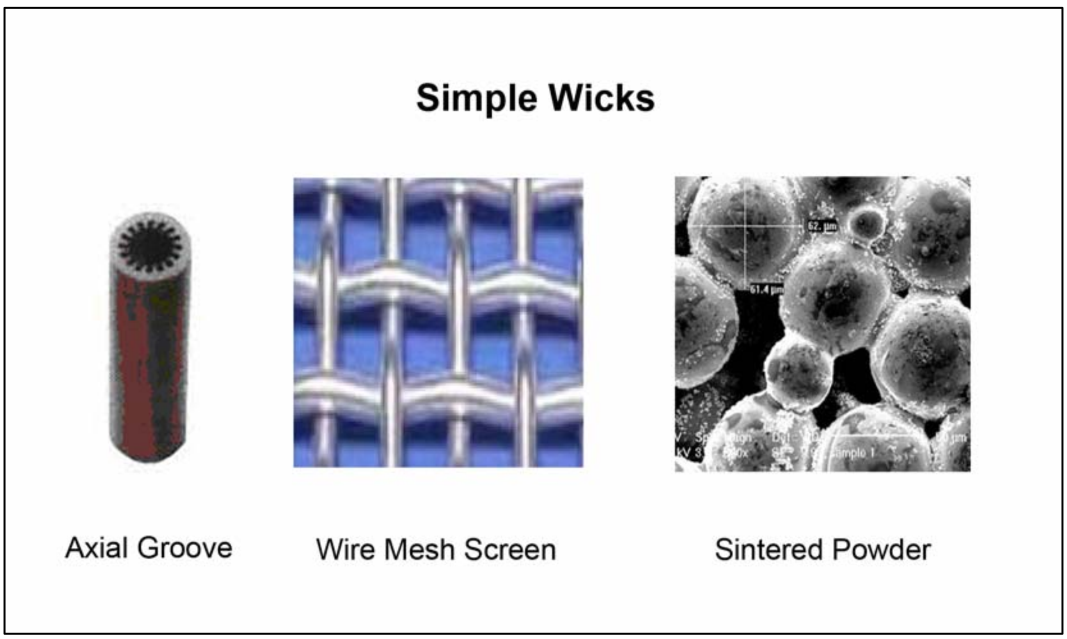

Modern heat pipes can contain any one single type of wicking structure or a combination of wicking structures to transport fluid from a high liquid pressure region to a low liquid pressure region. The permeability, K, of the wicking structure varies with its shape and design. Some examples of simple wicking structures are rectangular groove, wire mesh screen, and packed sintered powder. The rectangular groove wick is created by carving fine grooves into the interior core of the heat pipe. The wire mesh screen wick is composed of multiple layers of interwoven wires applied to the interior core of the heat pipe. The sintered powder wick consists of an arrangement of densely packed metal spheres along the interior core of the heat pipe.

C. The sections of the heat pipe

The heat pipe can be divided into three sections: the evaporator which is located near the heat source, the condenser which is located near the heat sink and the middle portion called the adiabatic section.

The evaporator section of the heat pipe is enclosed in a copper block, which is usually placed on top of the CPU. A thermal interface material (TIM) is placed between the block and the die to improve conduction of heat. The CPU's original heat conducts through the TIM, the block, and then through the walls of the heat pipe to a working fluid inside. The energy transported vaporizes the liquid. The pressure and temperature differences force the vapor to flow to the condenser, the cooler region of the heat pipe.

When the vapor reaches the condenser, it gives up its latent heat of vaporization, cools down and returns to its liquid state. At the condenser, heat is conducted through the heat pipe container, and then to the air by the process of natural convection. To enhance the rate of heat transfer to the environment, a heat exchanger can be used to increase the rate at which heat dissipates into the environment. In a heat pipe structure, a heat exchanger consists of a heat sink and a fan. The condensed working liquid then returns to the evaporator section through capillary action within the wick and completes the operating cycle.

D. Thermal resistance

In the search for a more efficient a heat pipe design, thermal resistance is often used as one of the key measures of overall performance. Thermal resistance defines the impedance to the transfer of heat when not heated uniformly.

In order to improve the heat pipe’s performance, its thermal resistance must be lowered as much as possible. One way this goal can be accomplished is by using measurements of heat pipes with various designs to statistically extrapolate the optimal design parameters such as powder size, wick thickness, material, working fluid, liquid charge, wick structure, shape, flatness, bend angle, diameter, and length. The effects of these parameters must be explored both individually and simultaneously. Unfortunately, both time and budget constraints prevent real-world testing of all the possible combinations of prototype heat pipes. Thus, a more feasible approach is needed to overcome these difficulties while still permitting the desired data to be collected and analyzed.

The answer to this problem is computer simulation. With certain assumptions taken, a mathematical model of heat pipes can be developed and simulated on computer. This computer model allows for the testing of many different possible factors that affects the heat pipe's thermal resistance without the costly and time consuming process of manufacturing and lab testing. Each factor that might affect the thermal resistance was simulated while holding the other factors constant and their effects on the thermal resistance can be interpolated from the trends when they are plotted against the thermal resistance values.

II. Statistical Analysis

A. Design of Experiments

1. 2^k Factorial Design

2. Center Points

3. Nested Design and Sub-sampling

4. Data Characteristics for Company C

5. Data Characteristics for Company B

6. Data Characteristics for Company A

B. Methods

1. Missing Data

2. ANOVA

Analysis of variance (ANOVA) is a procedure to determine whether differences exist between the means of two or more populations/factors. A factor can take on a certain number of values called levels and can either be discrete or continuous. For example, in data set B there were three factors: *powder size*, *wick thickness*, and *fluid charge*, where the first two factors had two levels each, and *liquid charge* had four levels. Each combination of factors and levels is called a cell.

The simplest ANOVA is called one-way ANOVA that compares the variation across the different levels of one factor. In multi-factor ANOVA, the objective is to determine significant factors in a model with multiple factors. There are two ways to model the multi-factor ANOVA (cell means and multi-factor). The distinction between these models is that the second model divides the cell means into an overall mean and factor effects. It makes the factor effect more explicit and it is a more emphasized approach than the cell means model.

In all instances, ANOVA makes the following assumptions: samples were selected at random from each population (or group), the data from each group are normally distributed, and all groups have the same standard deviation.

Different statistical software packages will invariably produce an ANOVA table with various calculations relating to the data. The most important part of the table is the p-value, which is the probability of observing the particular data sample in our experiment (or a more "extreme" data sample) given that there are no differences among the populations. A small p-value is an indication that there are significant differences among the populations. When looking at data set B's one-way ANOVA by treatment we observed a small p-value, which indicates there are significant differences among the various treatments. In the 3-factor analysis of data B, almost all the p-values were 0.05 or less. This shows us that the factors are all significant.

After checking the p-values to ensure all the variables in our best model are significant, we must look at residual plots to verify that our model is good and that none of the ANOVA assumptions have been violated. First, we will look for a pattern in our residuals, noting curvature or non-constant variance. Our assumptions of normality and constant variance of the data translate into assuming that the residuals are normally distributed with mean equal to zero and having a constant variance. Residuals also may indicate outliers and other issues with our data. For example, in data set B, we noticed non-constant variance and slight non-normality. However, it was unclear if the normality was seriously violated because departures from homogeneity of variance can lead to non-normality. Therefore, our model was good enough to continue analysis.

A possible remedy for non-normality or non-constant variance is using transformation on the data and then re-running the ANOVA. An appropriate transformation of a data set can often yield a data set that follows an approximately normal distribution. The Box-Cox transformation is a particularly useful family of transformations on a positive response and is defined as T(Y; λ) = (Y^2 - 1)/ λ if λ ≠ 0, and T(Y; λ) = *ln*(Y) if λ = 0, where Y is the response variable and λ is the transformation parameter. In order to find the optimal λ value, the Box-Cox transformation modifies the original data using the equations below for W_i, a standardized transformed variable. It then estimates the value of λ that minimizes the standard deviation of W_i where $W_i = (Y_i^{\lambda} - 1)/(\lambda G^{\lambda - 1})$ when $\lambda \neq 0$ and $W_i = G \ln(Y_i)$ when $\lambda = 0$. The Y_i s are the original data response values and G is the geometric mean of all the data. Most of the time using the suggested transformation will resolve the violations of our assumptions.

Overall, ANOVA gives us a way to initially look at the data and get a good feel for which model might be best by determining the significance of each factor. However, ANOVA only tests categorical independent variables. Later, we will redefine our independent variables from categorical to broader continuous variables and create a model using linear regression.

3. Tukey's Multiple Comparisons Procedure

Tukey's multiple comparisons procedure is used to investigate the differences among populations by providing confidence intervals for all pairwise differences between population means. This procedure assumes a balanced design—that is, the number of samples is the same for each population. In our case, we have balanced designs of either 3 or 6 tests per heat pipe for each experiment. Tukey's procedure is performed only if the Analysis of Variance (ANOVA) procedure finds that there are significant differences among populations. Because our *one-way* ANOVAs will turn out to be significant, we know that there are substantial differences among some heat pipes. Thus, we employ Tukey's procedure to find out which heat pipes are significantly different.

Tukey's method results in the following confidence interval for the pair-wise comparison of means: $(\overline{Y}_1 - \overline{Y}_2) \pm q_{\alpha(k,n-k)}\sqrt{\dfrac{MSE}{n}}$, where $\overline{Y}_i$ is the average of group i, MSE is the mean squared error, n is the common sample size, and q is the critical value of the "studentized range distribution" corresponding to k groups and $100(1-\alpha)\%$ confidence level. In our case, Tukey's test will be used to compare different treatments of heat pipes at the 95% confidence level (i.e $\alpha = 0.05$). We will then be able to group the treatments by ones that are statistically similar and ones that are statistically different, which will allow us to identify the top performing heat pipe combinations.

4. Regression

Regression analysis is a statistical tool for evaluating the relationship of one or more independent variables $x_1, x_2, \ldots, x_k$ to a single, continuous dependent variable y. Like ANOVA, regression assumes the independence and normality of observations and that the variance of y is the same for any x. In addition, regression assumes a specific model for the data. For example, a 2^k factorial design assumes a (near) linear relationship between the factors and the response variable. Thus, the regression model corresponding to a 2^k factorial design is

$$y_i = \beta_0 + \sum_{j=1}^{k} \beta_j x_{ij} + \varepsilon_i \,,$$

where y_i is the value of the response variable in the i^{th} trial, $\beta_0, \beta_1 \ldots, \beta_k$ are parameters, x_{ij} is the value of the independent variable x_j in the i^{th} trial, and ε_i is the unknown experimental error in the i^{th} trial. If this model is used for data set C, then the regression equation would be:

$$\theta_{(j-amb)i} \;=\; \beta_0 \;+\; \beta_1(\text{Wick Diameter})_i \;+\; \beta_2(\text{Wick Thickness})_i \;+\; \beta_3(\text{Liquid Charge})_i \;+\; \varepsilon_i$$

If interaction terms are added to the first–order model, then we have a model capable of representing some curvature in the response function:

$$y_i = \beta_0 + \sum_{j=1}^{k} \beta_j x_{ij} + \sum_{j<l} \sum \beta_{jl} x_{ij} x_{il} + \varepsilon_i$$

However, it is impossible to test whether or not there is a quadratic component in the relationship between a factor A and the response if A is only evaluated at two points

(.i.e. at the *low* and *high* settings). When one suspects that the relationship between the factors and the response are curvilinear, one can test for curvature (the presence of quadratic terms) in the model by adding replicates at the *center point*. This is illustrated in the diagram below for a 2^3 factorial design:

Figure II.15: Response surface with a center point

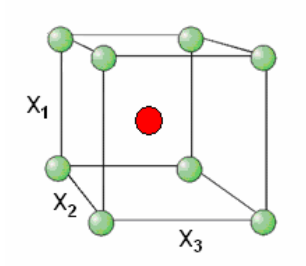

The addition of center points allows us to accomplish two goals, namely, to obtain a pure error estimate of the variance of the response, σ^2, and to test whether or not curvature is present in one or more of the factor effects. If curvature is present, the next step usually is to develop a full second-order model,

$$y_i = \beta_0 + \sum_{j=1}^{k} \beta_i x_i + \sum_{j<l} \sum \beta_{jl} x_{ij} x_{il} + \sum_{j=1}^{k} \beta_{jj} x_{ij}^2 + \varepsilon_i \, .$$

However, if the number of parameters in the model exceeds the number of observations, the parameters cannot be estimated. More observations must be added by augmenting the design with axial runs, as shown in Figure II.16 below. The resulting design is called a Central Composite Design.

Figure II.16: Central Composite Design for a two-factor experiment

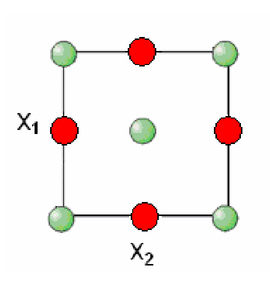

Usually, the center-point design is just the first step in a sequential experimental process to find a maximum or minimum of a response. After the initial experiment fails to detect a maximum/minimum, we search in a promising direction of steepest ascent/steepest descent until the response declines/increases. Once this occurs, we run another center-point design to confirm curvature and then run an augmented model to estimate the surface at the maximum/minimum.

C. Analysis

1. **Data Set for Company C**
2. **Data Set for Company B**
3. **Data Set for Company A**

D. Summary of Findings

1. **Data Set for company C**
2. **Data Set for Company B**
3. **Data Set for Company A**

E. Conclusion & Recommendations

Most of our analysis, including ANOVA and regression, can be considered preliminary. In addition, the design of experiments resulted in some serious violations of basic assumptions such as independence of observations. For example, by implementing nested design analysis we found that the repeated measurements taken from each heat pipe were actually correlated.

Furthermore, nested design revealed that there was a significant amount of variation in the manufacturing process for data sets B and C. This variation made it hard to tell whether the factors were really affecting the heat pipes performance or whether it was just the way the particular heat pipe was made. It would be best if in future experiments at least two of each heat pipe were built so as to account for some of the manufacturing variation.

While our regression estimates are statistically unbiased, they are based on extensive interpolation because we were only given one point inside the cube design. Thus, we would recommend that future experiments include additional observations. One possible design is a “composite design” as illustrated in figure II.45, where additional observations are taken at the red midpoints. Such a design would not only help increase the confidence level in the results, but it will also remedy the high correlations we encountered among some regression terms, enabling us to get a full quadratic fit of the response surface.

Figure II.45: Composite Design

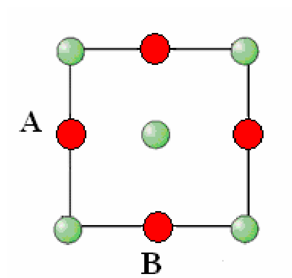

To allow for the extra runs suggested without greatly increasing the need for more heat pipes, it might be best to limit the number of factors in future experiments. In several cases, it would have been better to have fewer factors so more extensive analysis could have been done on the factors that were tested. For example, if one builds a tin heat pipe on Tuesday and an aluminum heat pipe on Friday and these two heat pipes are statistically different, then there is no way to draw a conclusion whether the metal type or the day of the week affected the heat pipe. This problem definitely arose in data set A, where in each *wick* category we had only 9 heat pipes but 5 factors to analyze.

We also noted that one factor that was set too low produced a heat pipe that did not work and it seemed that the high values of another factor always performed better. Using this information in the future, one could possibly set the values of the factors to a quantity that is known to work. This would trim down the number of factors, and one would be able to add the suggested additional runs without having to significantly increase the number of heat pipes in the experiment. Thus, we would recommend in all future experiments striking a balance between the amount of factors tested and the number of heat pipes in the experiment, keeping in mind that interaction terms must be taken into account.

On another note, consistency in data testing is a big part of having accurate statistics. Having actual data helps with the confidence of analysis instead of the low and high dichotomy.

III. Numerical Simulations

A. Mathematical Model

Mathematical modeling of a heat pipe can be quite complicated because the physical phenomena of the heat pipe requires a highly nonlinear system of partial differential equations in time, the spatial variables, velocity, temperature and pressure. Although our simulation assumes axial or cylindrical symmetry, the systems of partial differential equations that we apply can be used for bent or curved heat pipes. We use COMSOL software to find a finite element approximation to the solution of the system and perform numerical experiments on the model.

We make the following simplifying assumptions for our numerical simulations. We perform a stationary analysis where the temperature and the flows are in equilibrium. We assume the pipe is horizontal, thus ignoring the effect of gravity. We ignore radiation due to the low temperature difference in the heat pipe. We also assume that the wicking structure is located next to the cylindrical container, leaving a hollow corridor in the middle of the pipe through which the vapor can flow. Furthermore, we assume that vapor is not present in the wicking structure and that liquid is absent from the core of the pipe. Our computer simulation for this simplified steady state model serves as a foundation for more complicated and accurate time dependent simulations for later work.

Phenomenae and governing equations:

1. *Liquid flow and heat transfer in wick structure:*

PHENOMENA	VARIABLES	GOVERNING EQUATIONS

Phase change Liquid flow in wick structure Interfacial shear stress Liquid Entrainment Boiling Limitation	Temperature Pressure drop	Continuity Equation Darcy's Law Heat equation

2. *Liquid-vapor interface:*

PHENOMENA	VARIABLES	GOVERNING EQUATIONS
Capillary pressure Disjoining pressure Condensation	Temperature Pressure drop	Interfacial Mass Balance Interfacial Momentum Balance Clapeyron or Kelvin Equation

3. *Vapor flow:*

PHENOMENA	VARIABLES	GOVERNING EQUATIONS
Geometry effects Sonic limitations Mass diffusion	Temperature Pressure drop	Interfacial Mass Balance Van der Waals Equation Navier-Stokes equation

B. Software

We initially considered using MATLAB/Simulink for the numerical simulations. However, it became apparent that it would be too complicated and it would take too long to use MATLAB, especially when we had spent first half of semester to surveying literature. MATLAB was originally proposed because it is readily available, familiar to students and engineers and it had a finite element package. Nevertheless, it is still a mathematical package and setting up physical equations from basic mathematical functions is time-consuming and error-prone.

Comsol Multiphysics is a software package designed to model physical processes with many built-in equations which allowed us to concentrate on the physical phenomena instead of programming issues. Mathematical modeling for the cylindrical pipe is relatively easy as drawing and setting up equations are integrated into the software. There are also many options for visualization of the results as well as post-processing.

C. Geometry

We performed our simulations on a cylindrical heat pipe which was 170 mm in length. The dimensions for the evaporator, condenser and adiabatic sections are shown in Figure III.1.

Figure III.1: Baseline Dimensions

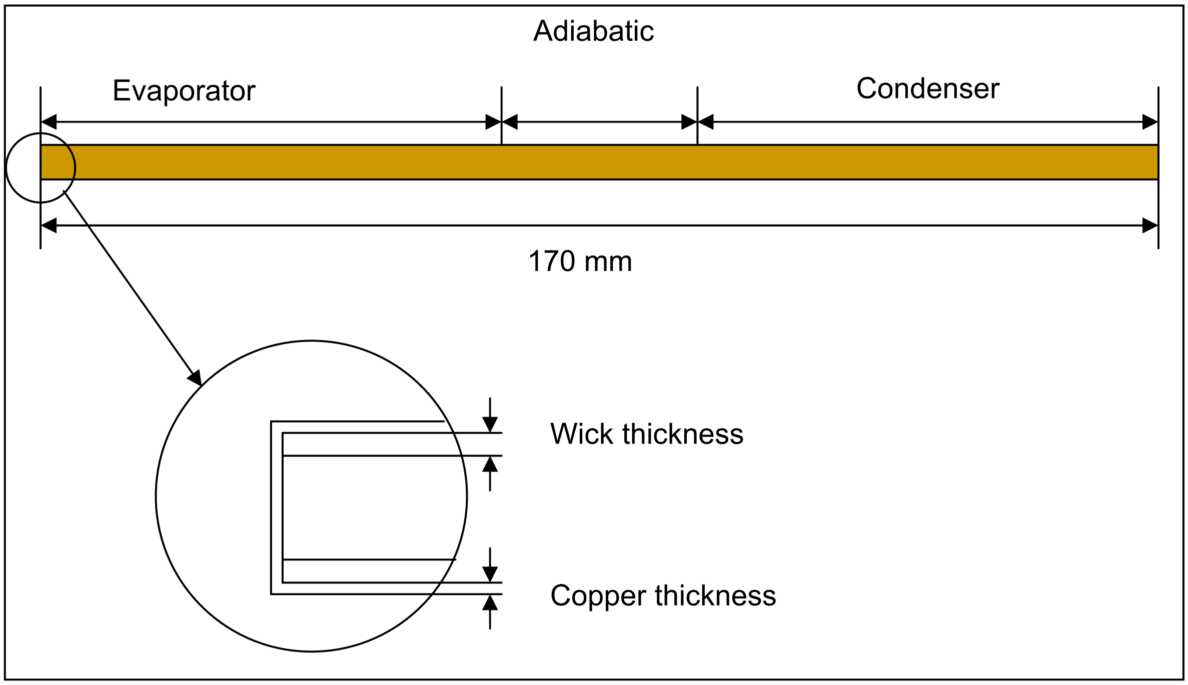

In subsequent diagrams, we only draw half of a lengthwise slice of the heat pipe. The pipe can be obtained by rotating the rectangle about its axis.

Figure III.2: Heat pipe diagram

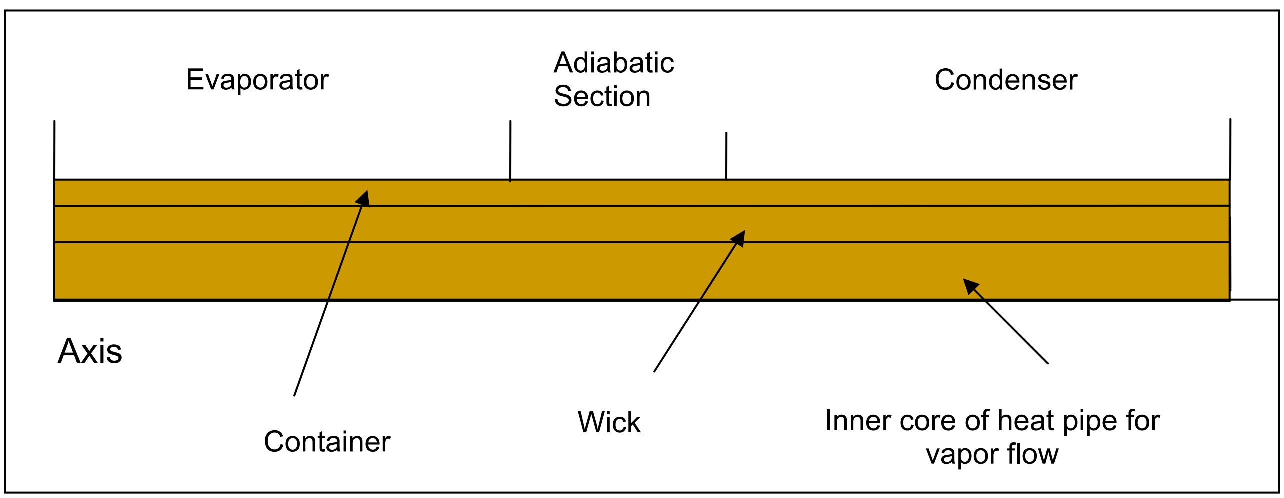

D. The PDE's

1. Fluid flow in the wick

To model the liquid flow, we used Brinkman's equation, a Navier-Stokes like system of equations used for fluid flow through a porous medium. Another model commonly used is Darcy's equation, a simpler equation which has its origins in flows through porous medium such as sand.

$$\rho \frac{\partial \mathbf{u}_2}{dt} - \nabla \cdot \eta \left(\nabla \mathbf{u}_2 + \left(\nabla \mathbf{u}_2 \right)^T \right) - \left(\frac{\eta}{K} \mathbf{u}_2 + \nabla p - \mathbf{F} \right) = \mathbf{0}$$

$$\nabla \cdot \mathbf{u}_2 = 0$$

The equations are written in terms of time t, the spatial variables, the density for the liquid ρ, the dynamic viscosity η, the permeability K, the pressure p, the velocity of the liquid $\mathbf{u}_2$ and any external forces $\mathbf{F}$, such as gravity.

2. Vapor flow through the center of the pipe

We use the Navier-Stokes equations to describe the vapor flow

$$\rho \frac{\partial \mathbf{u}_1}{dt} + \rho \left(\mathbf{u}_1 \cdot \nabla \right) \mathbf{u}_1 = \nabla \cdot \left[-p\mathbf{I} + \eta \left(\nabla \mathbf{u}_1 + \left(\nabla \mathbf{u}_1 \right)^T \right) - \left(\frac{2\eta}{3} - \kappa \right) \left(\nabla \cdot \mathbf{u}_1 \right) \mathbf{I} \right] + \mathbf{F}$$

$$\frac{\partial \rho}{\partial t} + \nabla \cdot \left(\rho \mathbf{u}_1 \right) = 0$$

where $\mathbf{u}_1$ is the velocity of the vapor, p is the pressure, η is the dynamic viscosity, κ is the dilatational viscosity, ρ is the density, and t is time.

3. Heat transfer in the pipe

We use the heat equation,

$$\rho C \frac{\partial T}{\partial t} + \nabla \cdot \left(-k \nabla T \right) = Q - \rho C \mathbf{u} \cdot \nabla T$$

ignoring radiation, to describe heat transfer in the pipe where *C* is the heat capacity of the vapor, *T* its temperature, *t* is time and *k* is the heat conductivity.

E. Boundary Conditions

Rotating the rectangle below about its axis will produce a cylindrical heat pipe. The external boundaries are at the ends and on the pipe as well as on the container

1. Boundary conditions for the Navier-Stokes equations in the center of the pipe (vapor flow)

Figure III.3

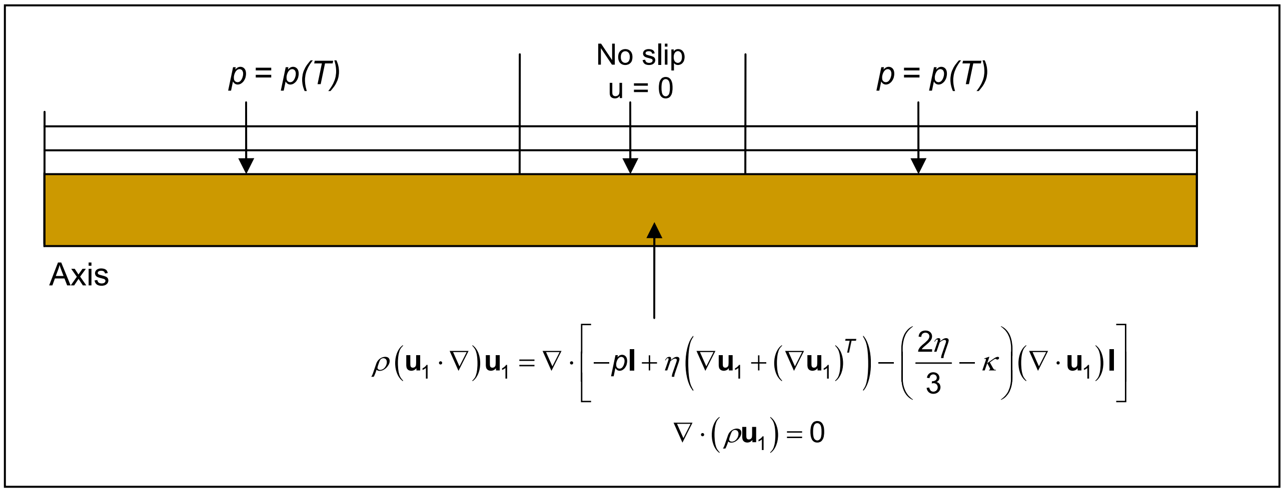

The saturated vapor pressure, *p(T)*, at temperature T is given by VaporPressure(T) as defined in section III.F. The difference of saturated vapor pressure between the evaporator and condenser drives the vapor flow from evaporator to condenser. The vapor flow velocity at the interface with water flow in the adiabatic section is zero due to friction with the wick structure and water (no slip).

2. Boundary condition for Brinkman equations (liquid water flow)

Figure III.4

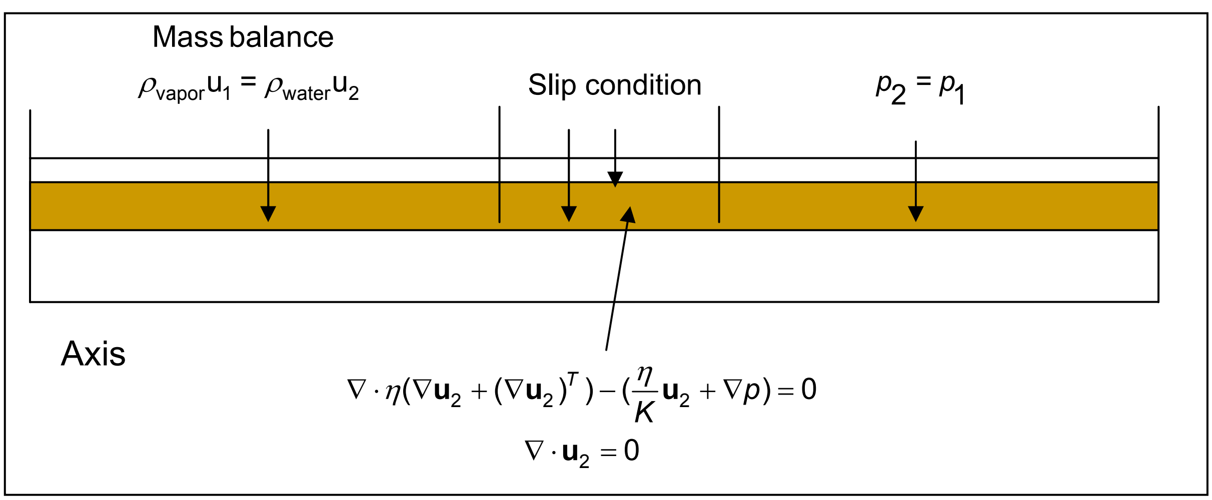

Due to flooding at the condenser, the water pressure is equal to the vapor pressure ($p2 = p1$). On the other hand, at the evaporator, the water pressure is lower than the vapor pressure because of capillary pressure (Peterson). The exact pressure at the evaporator is dependent on the water flow; thus, we cannot set the boundary condition as pressure. However, the water flow is related to the vapor flow, therefore the boundary condition is the mass balance equation. The water velocity at the boundary in the adiabatic section is tangent to the surface (slip condition); unlike vapor, water velocity is not zero because it has higher density and loses little velocity due to friction.

3. Boundary condition for heat transfer in the heat pipe

Figure III.5

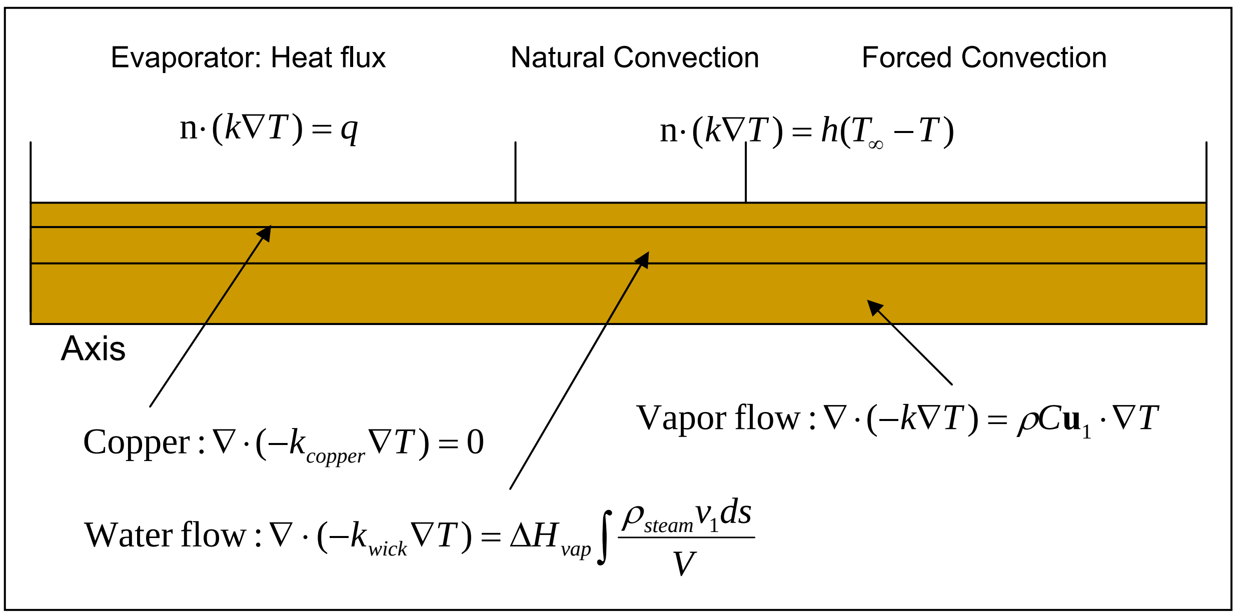

At the copper cover, the only heat transfer is due heat conduction. To simplify the simulation, we have Comsol Multiphysics treat the copper cover as a highly conductive layer, which uses a similar equation:

$$\nabla\cdot(-d_s k_{copper}\nabla T)=q_{\partial\Omega}-q_{\Omega}$$

where d_s is the layer thickness, $q_{\partial\Omega}, q_{\Omega}$ are heat flux from boundary to layer (copper cover) and from layer to subdomain (the wick structure).

Heat transfer in the vapor flow is due to both heat conduction and convection. The equation for vapor flow has the convective term $\rho C\mathbf{u}_1 \cdot \nabla T$ to account for convection. The water flow is slow enough to ignore convection term. However, we have a heat source or heat sink term to simulate heat gained or lost due to the phase change at the condenser and evaporator. The heat gained or lost is proportional to the rate of mass evaporated or condensed, calculated by the integral $\int \frac{\rho_{steam} v_1 ds}{V}$ at the interface between water and vapor.

The boundary condition at the evaporator is given by the heat flux, $\mathrm{n}\cdot(k\nabla T) = q$, where a value of q between 30,000 and 50,000 W/m^2 is needed to simulate the heat flux of a 30-50 W chip. The boundary condition for the adiabatic and the condenser section is natural convection and forced convection respectively, described by $\mathbf{n}\cdot(k\nabla T) = h(T_\infty - T)$ where the heat transfer coefficient h is about 12 W/Km^2 for natural convection and is about 1200 W/Km^2 for forced convection .erical Simulation

In these equations, properties such as density, viscosity, pressure change with temperature. Formulae for water and steam properties published by the International Association for the Properties of Water and Steam (IAPWS) could be used for best accuracy. However, it is difficult to implement and not necessary for our model. In our model, we used the following empirical equations:

- Thermal conductivity of steam[1]

$$\mathrm{kSteam}(T) = 10^{1.7186(T)^2 - 7.8203\log(T) + 7.1242}$$

- Density of saturated steam

$$\mathrm{rhoSteam}(T) = \frac{1.322828963 \times 10^{\left(\frac{7.5(T-273)}{-35.3+T}\right)}}{T} \qquad (1)$$

[1] From Comsol Multiphysics library

- Vapor Pressure at T (Vomel)

$$\text{VaporPressure}(T) = 611 \times 10^{\left(\frac{7.5(T-273)}{-35.3+T}\right)}$$

- Heat capacity of steam[1]

$$\text{CpSteam}(T) = -0.0002T^2 + 0.7929T + 1673.1$$

- Dynamic viscosity of steam[1]

$$\text{etaSteam}(T) = 0.9174 \times 10^{-12} T^2 + 0.3881 \times 10^{-7} T - 0.2102 \times 10^{-5}$$

- Dynamic viscosity of water[1]

$$\text{etaWater}(T) = 0.334 \times 10^{-9} T^4 - 0.457 \times 10^{-6} T^3 + 0.236 \times 10^{-3} T^2 - 0.054T + 4.67$$

- Permeability (Peterson)

$$K = \frac{D^2 \varphi^3}{150 \cdot (1-\varphi)^2}$$

where D is the powder size or diameter of the spheres, φ is the porosity which is determined empirically.

Equation (1) is derived from ideal gas law $pV = nRT$ where p is the vapor pressure. We attempted to use the Van der Waals for more accurate results but we found that both gave similar values of the density (at low pressure) while the ideal gas law equation is much simpler to implement in Comsol Multiphysics. We prefer the empirical formula for vapor pressure to the theoretical Clausius-Clapeyron equation because the Clausius-Clapeyron equation does not give an accurate value of the vapor pressure. We assume that the water density is constant as the change is small enough to ignore.

We simulate the model with different values of a parameter while keeping other parameters constant to investigate the dependence of the thermal resistance on each parameter. From information obtained from the numerical experiments, engineers might be able to make more informed decisions in heat pipe design.

[1] Comsol Multiphysics library

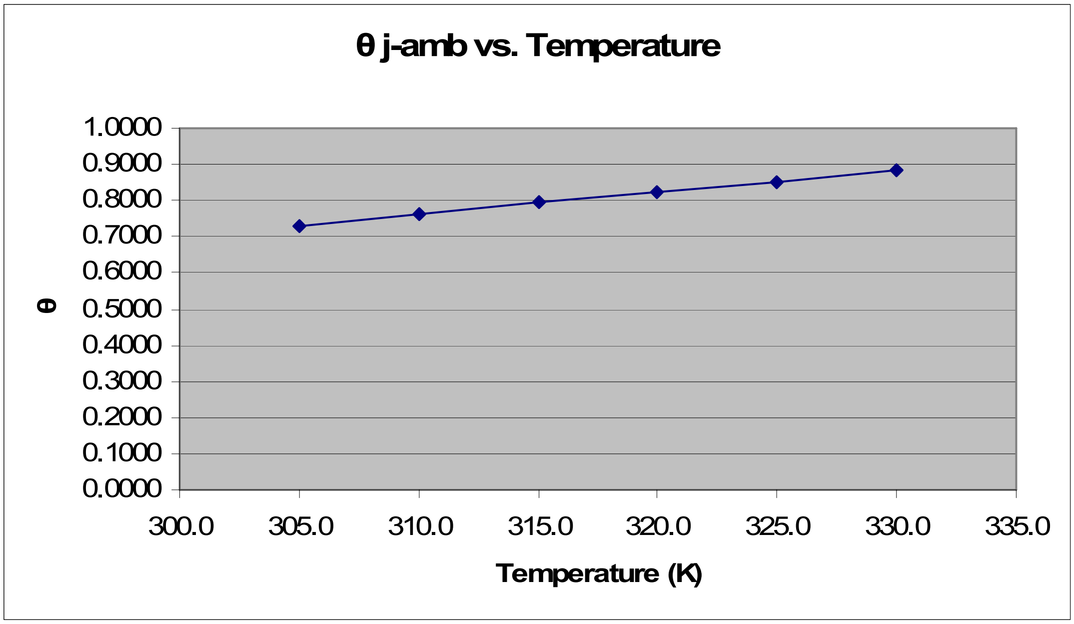

The graph shows theta increases as temperature at the evaporator increases. Engineers should keep this in mind when designing a cooling system using heat pipe. The temperature might be higher than expected if they assume the thermal resistance, θ, is constant.

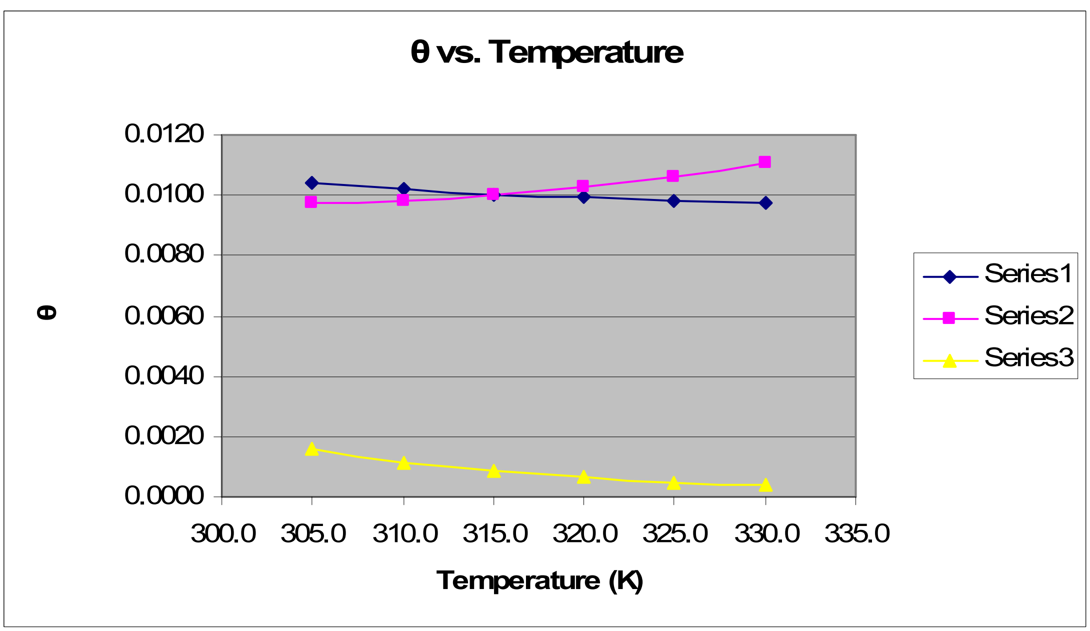

The simulation also allows us to look at how theta of each section responds to the temperature increase. The graph shows the θ_{evap} (series 1) and θ_{adia} (series 3) section decreases while θ_{cond} (series 2) increases.

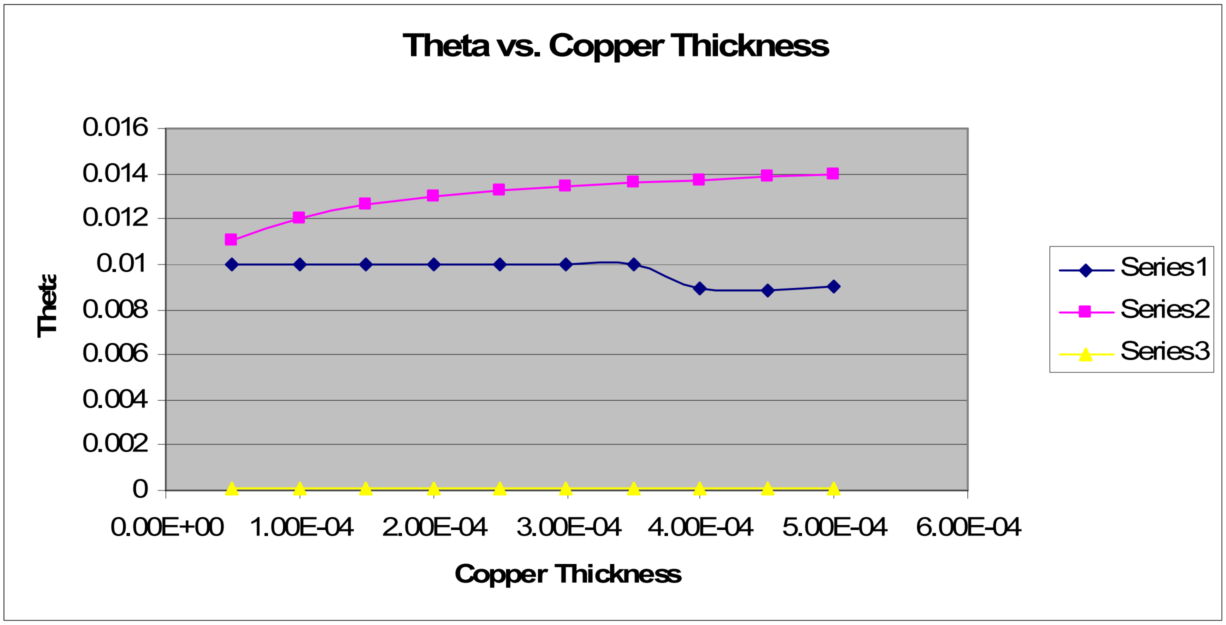

This graph shows θ also responds differently to copper thickness change. From the graph, we surmise that a heat pipe might perform better if the copper thickness is thinner at the condenser (series 2) and thicker at the evaporator (series 1).

Analysis and Limitations of Model

This model has some limitations that should be addressed. The model assumes that there is no vapor in wick structure, which is not true, especially when intense boiling or dry-out occurs. At high temperature or heat flux, vapor will occupy almost all the wick structure at evaporator due to intense boiling. In that case, the heat transfer and water flow will change dramatically and the model fails to take in account this. In the dry-out case, the model could not take into account the limitation of capillary pressure. The pressure drop at the evaporator drives the water flow in the wick structure but it has a maximum value, which could be calculated by $\frac{2\sigma}{.41r_s}$ [Peterson]. In the model, the pressure at the evaporator could be any value and we only know there is dry-out in the heat pipe if the pressure drop exceeds the aforementioned value. In both cases, the assumption that vapor is absent in wick structure means that the model will fail to predict performance at a high temperature or heat flux. Nevertheless, the model serves as a foundation for further development and can predict the performance at low temperature or heat flux, where the assumption is acceptable.

IV. Conclusions and Recommendations

In order to find optimal design parameters to minimize thermal resistance, we recommend a dual approach – first, a numerical simulation to find theoretical optimal values of the design parameters, followed by manufacturing trials and statistical analysis.

A more accurate model needs to be developed, one that reflects the true geometry of the the heat pipes in production. One advantage of the finite element method is its ability to handle curved boundaries. Also, the assumption that vapor and liquid do not mix in the pipe should be eliminated. A more thorough numerical experimentation is needed; the effects of the combined changes in different design parameters should be investigated. To take into account the limitation of capillary pressure and change in water flow, we can use a moving mesh for the water flow. The moving mesh in Comsol Multiphysics allows us to model dynamic water-vapor boundary instead of the static one that we used. To take in account the change of heat transfer due to intense boiling, a two-phase heat transfer is better than the current model.

Several things will greatly impact future statistical analysis of empirical data. Most importantly, one could build two of each type of heat pipe without this information it is impossible to move beyond preliminary analysis. Second, trimming down the number of factors in each experiment will greatly reduce the number of heat pipes needed. Third, axial runs should be included so as to prevent problems with correlation and to achieve a better fit a curved surface to the data with a more accurate minimum. In the current setting, there were many limitations on the analysis one could perform because of the limited number of heat pipes.

References

COMSOL User's Guide, September 2005.

Faghri. Amir, Heat Pipe Science and Technology, Taylor and Francis, New York, NY, 1995.

DiStefano, Eric, H. Pokharna, S. V. Machiroutu, "Raising the Bar for Heat Pipes in Notebook Cooling", 13th International Heat Pipe Conference, Shanghair, China, September, 2004.

Garner, Scott. "Heat pipes for electronics cooling applications". http://www.electronics-cooling.com/Resources/EC_Articles/SEP96/sep96_02.htm

Kleinbaum DG, Kupper LL, Muller, KE, and Nizam A. *Applied Regression Analysis and Other Multivariable Methods*, 3rd Edition. Duxbury Press, Pacific Grove, CA, 1998. (pp. 389-404).

Kutner MH, Nachtsheim CJ, Neter J, Applied Linear Regression Models, 4th Edition. Irwin/McGraw-Hill, New York, NY, 2003. (pp. 368)

Ma, Hongbin. "Highly Efficient Heat Pipes".

Learning Matlab, The MathWorks, Inc. 2002

Minitab Technical Support Document, Calculations for the Box-Cox Transformation in Minitab, http://www.minitab.com/support/docs/BoxCoxTransformCalculations.pdf, March 31, 2006.

Montgomery, D.C., *Design and Analysis of Experiments*, New York: John Wiley & Sons, Inc., 1976 and 1991.

Narayanan K.R., Shankara. "What is a Heat Pipe?" The Chemical Engineers' Resource Page. 2004. http://www.cheresources.com/htpipes.shtml

Nave, R. "Capillary Action." HyperPhysics. http://hyperphysics.phy-astr.gsu.edu/hbase/surten2.html

NIST/SEMATECH e-Handbook of Statistical Methods, http://www.itl.nist.gov/div898/handbook/, March 31, 2006.

"The Perkins Family" The Building Engineering Services Heritage Group. 2003. http://www.hevac-heritage.org/victorian_engineers/perkins/perkins.htm.

Peterson, G.P., An Introduction to Heat Pipes, Modeling, Testing and Applications, John Wiley & Sons, Inc, New York, New York, 1994.

Sall, Lehman, Creighton, JMP Start Statistics, California: Duxbury, 2001

S-Plus Guide to Statistics Vol. 1, Seattle, Washington: Insightful Corporation, 2001

Zhang, J.S., Design of Experiments (DOE), Rutgers, The State University of New Jersey, http://www.stat.rutgers.edu/~jszhang/stat/DOE.html, March 24, 2006.

Appendix A. Numerical simulation data

For the tables in this appendix, θ, is calculated by the following formulae:

$$\theta_{j-amb} = \frac{T_{\max} - T_{cond}}{P}$$
$$\theta_{evap} = \frac{T_{\max} - T_4}{P}$$
$$\theta_{adia} = \frac{T_4 - T_5}{P}$$
$$\theta_{cond} = \frac{T_5 - T_{cond}}{P}$$

where T_4 and T_5 are the temperature at point 4 and 5 (two ends of adiabatic section) in the following diagram.

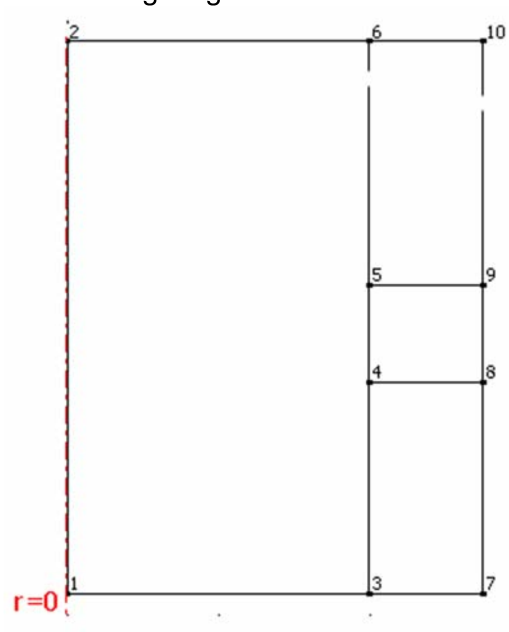

Tmax is the maximum temperature at the evaporator and Tvapor is the average temperature of the vapor in the heat pipe.

HeatFlux	Power	Tmax	Tvapor	T4	T5	Tcond	Thetaevap	ThetaCond	Thetaadia	Theta
1804.9429	34.0225	330.0000	329.5476	329.6675	329.6549	329.2789	0.0098	0.0111	0.0004	0.8818
1560.7182	29.4189	325.0000	324.6118	324.7109	324.6967	324.3843	0.0098	0.0106	0.0005	0.8498
1290.6896	24.3290	320.0000	319.6801	319.7588	319.7433	319.4933	0.0099	0.0103	0.0006	0.8221
1001.4644	18.8772	315.0000	314.7510	314.8104	314.7943	314.6057	0.0100	0.0100	0.0009	0.7946
694.5380	13.0918	310.0000	309.8248	309.8662	309.8511	309.7229	0.0102	0.0098	0.0012	0.7638
364.8043	6.8764	305.0000	304.9049	304.9282	304.9174	304.8503	0.0104	0.0098	0.0016	0.7271

Table A.1: Data collected from temperature at evaporator parameter simulation

HeatFlux	Power	Tmax	Tvapor	T4	T5	Tcond	Thetaevap	ThetaCond	Thetaadia	Theta
45000.0000	55.1351	357.1619	356.3802	356.6241	356.6208	355.8919	0.0098	0.0132	0.0001	1.0368
40000.0000	49.0090	343.6552	342.9769	343.1706	343.1639	342.6114	0.0099	0.0113	0.0001	0.8908
35000.0000	42.8828	334.5660	333.9846	334.1389	334.1293	333.6954	0.0100	0.0101	0.0002	0.8061
30000.0000	36.7567	328.2796	327.7853	327.9098	327.8986	327.5453	0.0101	0.0096	0.0003	0.7694
25000.0000	30.6306	322.9097	322.4983	322.5974	322.5848	322.2992	0.0102	0.0093	0.0004	0.7479
20000.0000	24.5045	317.8861	317.5552	317.6316	317.6180	317.3946	0.0104	0.0091	0.0006	0.7299
15000.0000	18.3784	313.0855	312.8336	312.8900	312.8761	312.7110	0.0106	0.0090	0.0008	0.7120
10000.0000	12.2522	308.4968	308.3240	308.3625	308.3497	308.2399	0.0110	0.0090	0.0010	0.6935
5000.0000	6.1261	304.1305	304.0400	304.0611	304.0521	303.9962	0.0113	0.0091	0.0015	0.6742

Table A.2: Data collected from heat flux parameter simulation

Radius	HeatFlux	Power	Tmax	Tvapor	T4	T5	Tcond	Thetaevap	ThetaCond	Thetaadia	Theta
3.25E-03	30000	36.75672	326.7512	326.2423	326.386	326.378	326.0451	0.009936	0.009057	0.000218	0.727791
3.00E-03	30000	36.75672	328.2796	327.7853	327.9098	327.8986	327.5453	0.010061	0.009612	0.000305	0.769372
2.75E-03	30000	36.75672	326.9583	326.4809	326.5832	326.5672	326.2267	0.010205	0.009263	0.000436	0.733425

Table A.3: Data collected from pipe radius parameter simulation

Porosity	HeatFlux	Power	Tmax	Tvapor	T4	T5	Tcond	Thetaevap	ThetaCond	Thetaadia	Theta
0.9500	2911.1471	54.8740	360.8529	359.5070	359.7761	359.7734	358.2755	0.0196	0.0273	0.0000	1.1090
0.9000	2916.6648	54.9780	357.1700	356.3778	356.6217	356.6185	355.8895	0.0100	0.0133	0.0001	1.0399
0.8500	2919.3747	55.0290	354.6995	354.1008	354.3310	354.3274	353.8573	0.0067	0.0085	0.0001	0.9940
0.8000	2921.1375	55.0623	352.8303	352.3319	352.5527	352.5487	352.2066	0.0050	0.0062	0.0001	0.9595
0.7500	2922.4194	55.0864	351.3409	350.9045	351.1181	351.1138	350.8474	0.0040	0.0048	0.0001	0.9320
0.7000	2923.4078	55.1051	350.1192	349.7249	349.9327	349.9281	349.7113	0.0034	0.0039	0.0001	0.9095
0.6500	2924.1968	55.1199	349.1007	348.7367	348.9397	348.9349	348.7530	0.0029	0.0033	0.0001	0.8908
0.6000	2924.8390	55.1320	348.2468	347.9059	348.1049	348.1000	347.9439	0.0026	0.0028	0.0001	0.8751
0.5500	2925.3648	55.1420	347.5384	347.2157	347.4113	347.4062	347.2697	0.0023	0.0025	0.0001	0.8621
0.5000	2925.7900	55.1500	346.9749	346.6667	346.8597	346.8545	346.7333	0.0021	0.0022	0.0001	0.8518

Table A.4: Data collected from porosity parameter simulation

Layer (Copper Thickness)	HeatFlux	Power	Tmax	Tvapor	T4	T5	Tcond	Thetaevap	ThetaCond	Thetaadia	Theta
5.00E-05	2926.032	55.155	348.180	347.360	347.628	347.623	347.011	1.00E-02	1.11E-02	9.077E-05	0.874
1.00E-04	2922.528	55.088	352.199	351.390	351.648	351.644	350.980	9.99E-03	1.21E-02	7.540E-05	0.948
1.50E-04	2920.108	55.043	354.532	353.731	353.983	353.979	353.284	9.98E-03	1.26E-02	6.718E-05	0.991
2.00E-04	2918.228	55.007	356.076	355.280	355.527	355.524	354.809	9.98E-03	1.30E-02	6.213E-05	1.019
2.50E-04	2916.664	54.978	357.176	356.383	356.627	356.624	355.895	9.98E-03	1.33E-02	5.874E-05	1.040
3.00E-04	2915.304	54.952	358.001	357.212	357.453	357.450	356.710	9.98E-03	1.35E-02	5.629E-05	1.055
3.50E-04	2914.084	54.929	358.644	357.856	358.096	358.093	357.345	9.97E-03	1.36E-02	5.445E-05	1.068
4.00E-04	2912.966	54.908	359.100	358.370	358.608	358.605	357.851	8.96E-03	1.37E-02	5.301E-05	1.076
4.50E-04	2911.925	54.889	359.510	358.787	359.024	359.021	358.261	8.86E-03	1.38E-02	5.187E-05	1.084
5.00E-04	2910.945	54.870	359.860	359.130	359.366	359.363	358.599	9.00E-03	1.39E-02	5.095E-05	1.091

Table A.5: Data collected from copper thickness parameter simulation

Appendix B: Graphs

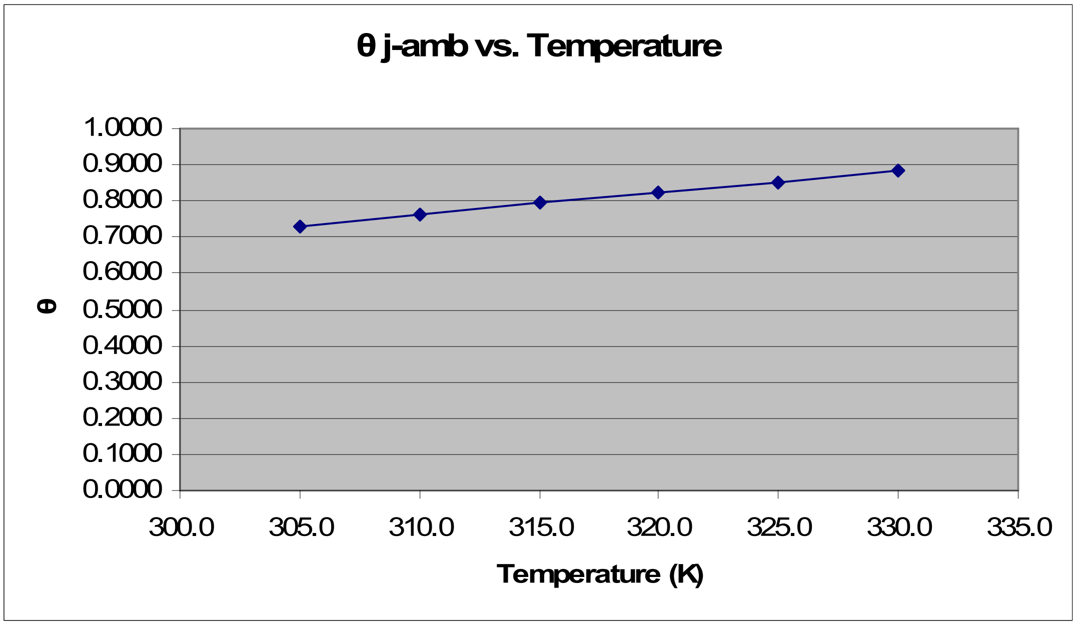

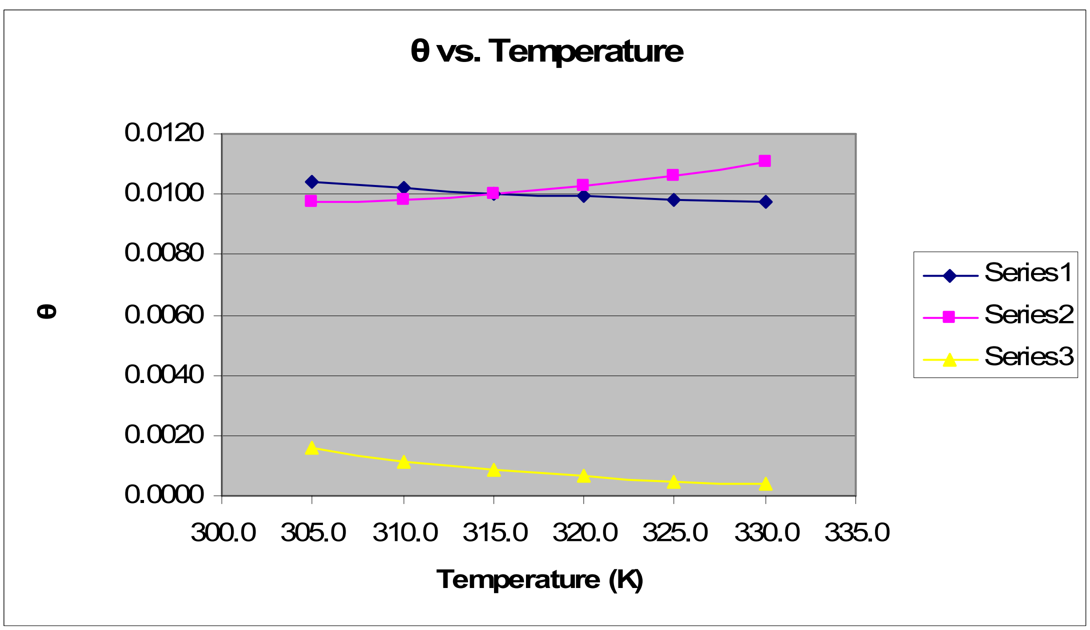

Series 1: θ evap
Series 2: θ cond
Series 3: θ adia

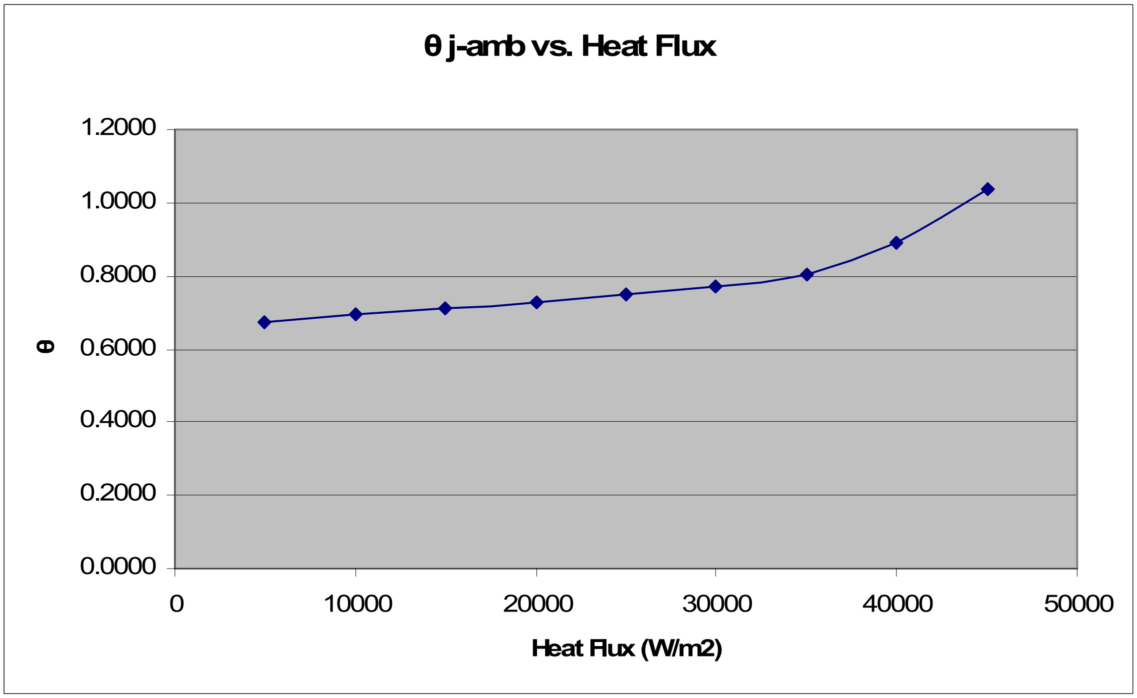

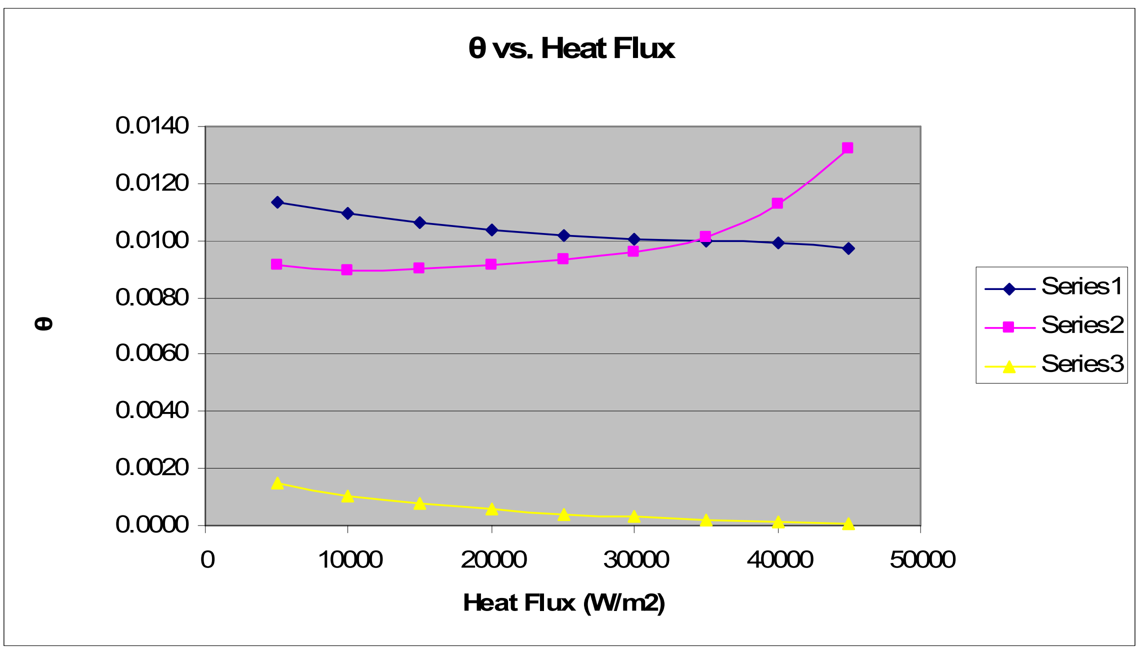

Series 1: θ evap
Series 2: θ cond
Series 3: θ adia

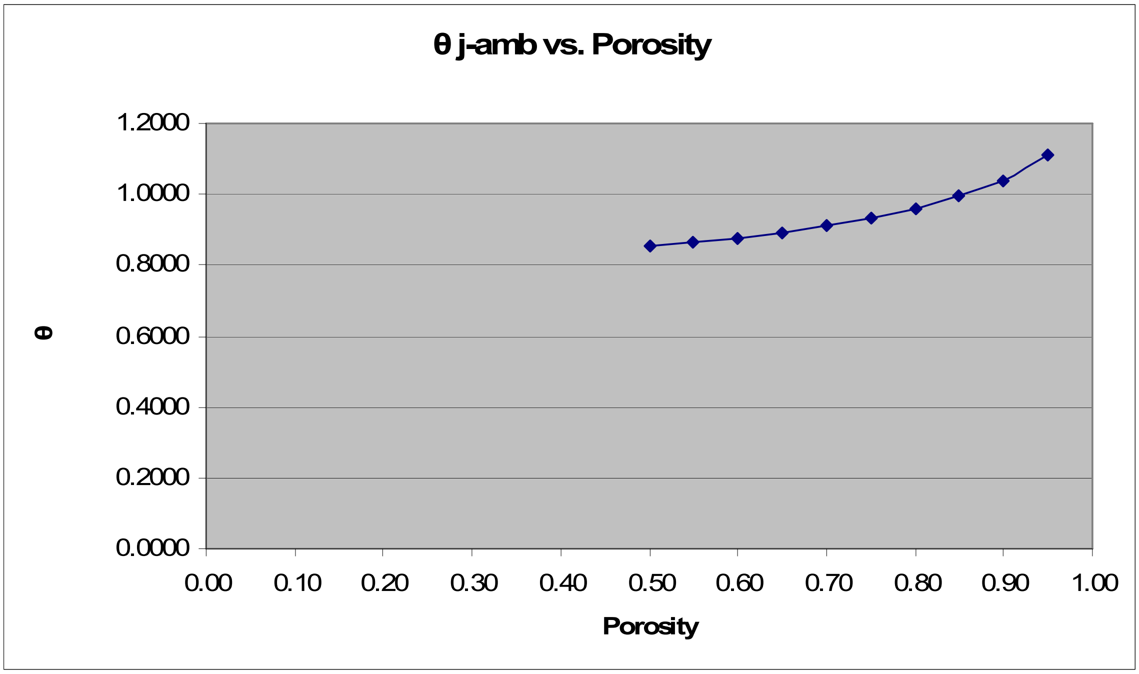

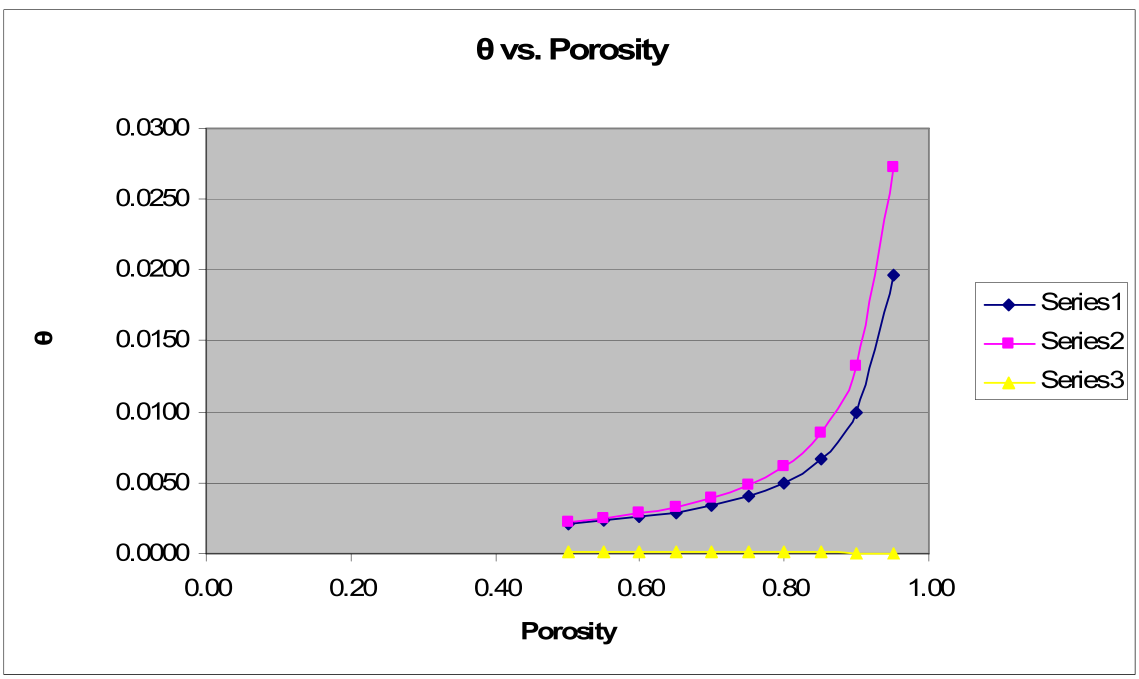

Series 1: θ evap
Series 2: θ cond
Series 3: θ adia

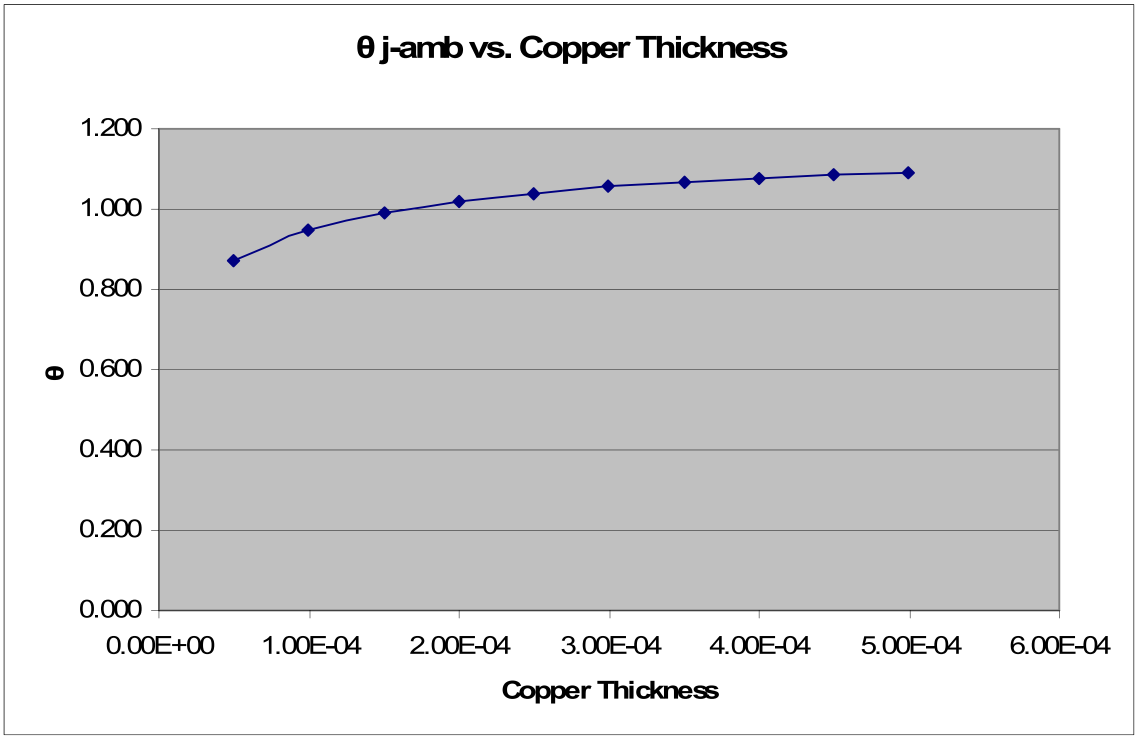

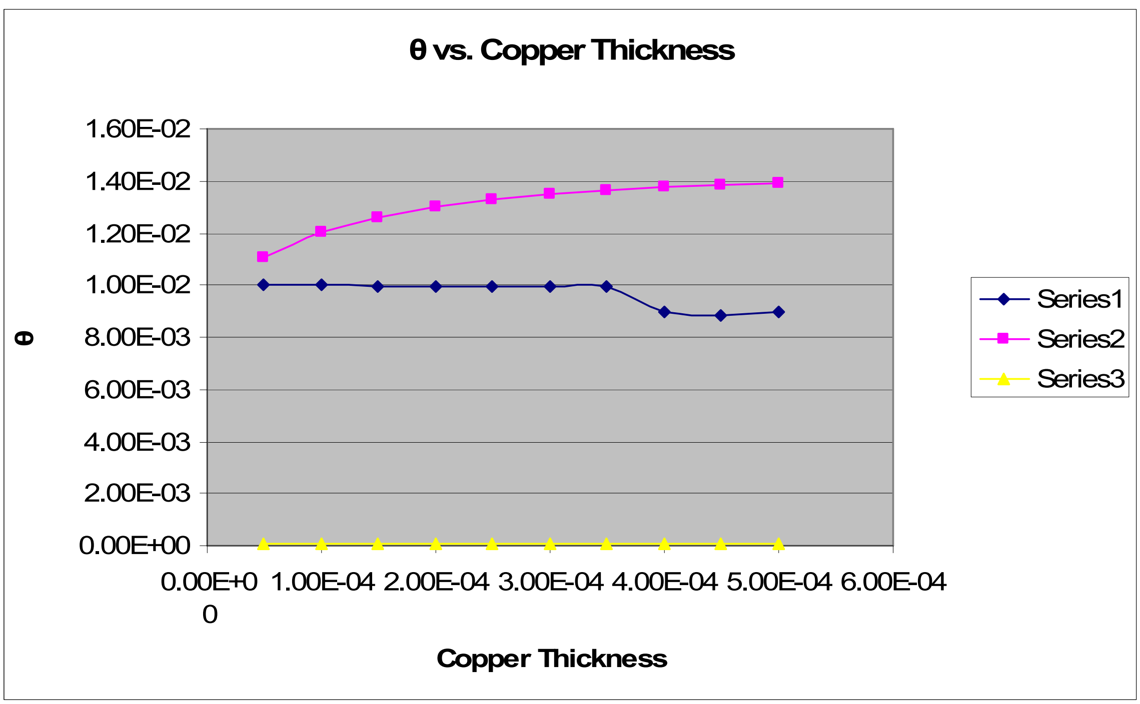

Series 1: θ evap
Series 2: θ cond
Series 3: θ adia

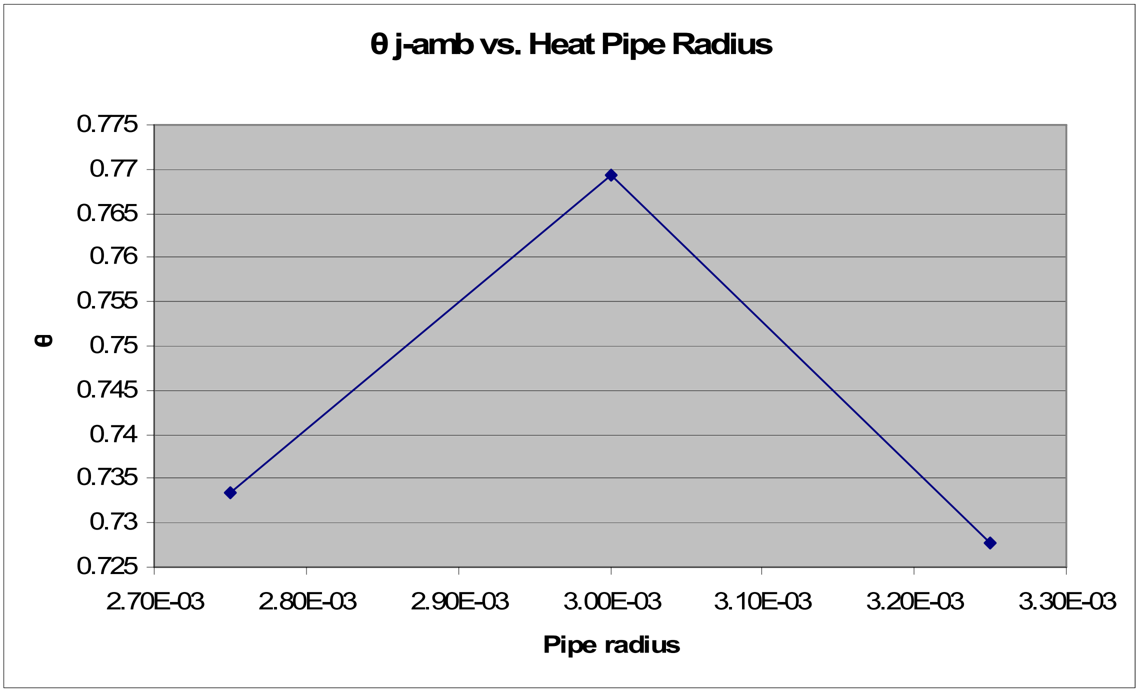

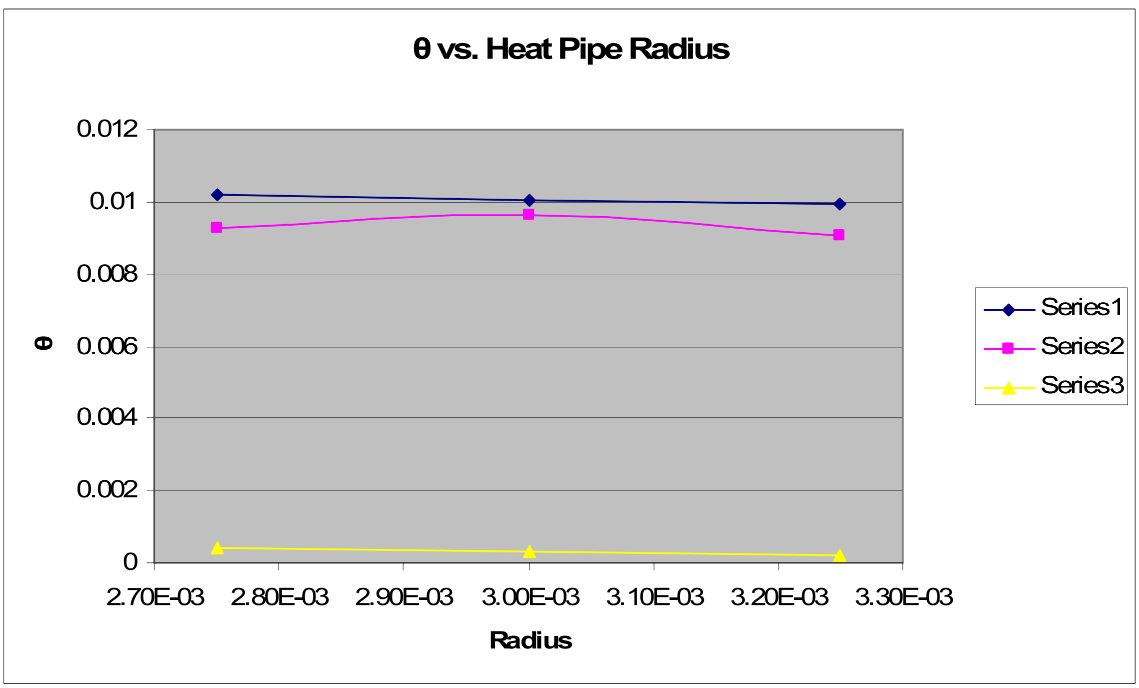

Series 1: θ evap
Series 2: θ cond
Series 3: θ adia